Japanese Journal of Applied Physics

The Japan Society of Applied Physics

REGULAR PAPER

Proposal and numerical verification of an ultrasmall terahertz source using integrated photonic crystal waveguides for highly efficient differential frequency generation

To cite this article: Yota Koyama *et al* 2023 *Jpn. J. Appl. Phys.* **62** SG1033

Japanese Journal of Applied Physics **62**, SG1033 (2023) **REGULAR PAPER**
https://doi.org/10.35848/1347-4065/acc18d

Proposal and numerical verification of an ultrasmall terahertz source using integrated photonic crystal waveguides for highly efficient differential frequency generation

Yota Koyama[1], Hisaya Oda[2], Naoki Ikeda[3], Yoshimasa Sugimoto[3], and Nobuhiko Ozaki[1*]

[1]*Faculty of Systems Engineering, Wakayama University, Wakayama 640-8510, Japan*
[2]*Chitose Institute of Science and Technology, Chitose, Hokkaido 066-8655, Japan*
[3]*National Institute for Materials Science, Tsukuba, Ibaraki 305-0047, Japan*

[*]E-mail: ozaki@wakayama-u.ac.jp

Received December 20, 2022; revised February 26, 2023; accepted March 6, 2023; published online March 23, 2023

We propose and numerically investigate integrated photonic crystal waveguides (PhC-WGs) formed in a semiconductor slab to realize an ultrasmall and highly efficient terahertz (THz) wave source. The structure consists of a straight PhC-WG with low-group-velocity and low-dispersion (LVLD) for efficient difference frequency generation (DFG) connected to two PhC-WGs to introduce two fundamental lights into the LVLD PhC-WG. The fundamental light propagating through each PhC-WG designed to enhance their electric fields by the slow-light effect is efficiently coupled to the LVLD PhC-WG owing to the reduced refractive index differences at the boundaries of the heterostructures. The DFG from the two fundamental lights was numerically simulated, and a temporal intensity oscillation corresponding to the difference in frequency was clearly observed. By comparing the DFG intensities of the integrated structures with an LVLD PhC-WG and a strip WG, the estimated DFG intensity from the LVLD PhC-WG was more than 100 times higher than that from the strip WG. These results indicate the effectiveness of the proposed heterostructure in the application of a highly efficient THz source with an ultrasmall footprint compared with conventional materials.

1. Introduction

Terahertz (THz)-wave technologies have been extensively studied for various applications[1–4] such as spectroscopic sensing, nondestructive imaging, and telecommunications. For these applications, various THz-wave generation methods have been developed.[5–16] Among these, optical to THz-wave conversion methods using a nonlinear optical (NLO) effect, for example, difference frequency generation (DFG), have been attractive because of their practical features, including tunability and room-temperature operation.[9] However, the THz-DFG equipment, including external high-power fundamental light sources, tends to be bulky owing to the limitations of available NLO crystals and their DFG efficiency. Therefore, the development of highly efficient THz-DFG media is necessary to miniaturize the THz sources.

To meet this requirement, we previously reported a THz-DFG using a two-dimensional (2D) photonic crystal waveguide (PhC-WG),[17] which is realized by a line defect in periodic air-hole arrays perforated in a slab of Ga(Al)As.[18] By using the III-V semiconductor, a relatively large second-order nonlinear electric susceptibility ($\chi^{(2)}$) can be obtained owing to the lack of inversion symmetry of the crystal.[19] In addition, the extremely strong light confinement in the PhC-WG enhances the light–matter interaction and NLO effects.[20–22] Furthermore, the line defect mode in the photonic bandgap provides a unique dispersion relation that can be controlled by the structural parameters of air holes.[23] We performed structural modifications of the PhC to realize a low-group-velocity and low-dispersion (LVLD) waveguide mode,[17,24] enabling the enhancement of the electric fields of fundamental light and satisfying their phase-matching condition. On the basis of these advantages, a highly efficient DFG of THz-wave in an LVLD PhC-WG was demonstrated.[17] However, the LVLD PhC-WG still has the issue of introducing fundamental light; the coupling efficiency of the external light should be lowered because of the low-group velocity (high refractive group index) of the PhC-WG. To address this issue, we devised and investigated integrated PhC-WGs in heterostructures.[25]

The heterostructure consists of an LVLD PhC-WG connected to two standard (STD) PhC-WGs. The STD PhC-WGs contain light-emitting materials that generate fundamental light, and the slow-light in the waveguide modes is set to correspond to each fundamental light wavelength. These contrivances improved the coupling efficiency of the LVLD PhC-WG. In addition, the footprint of the source device can be significantly reduced because a fundamental light source can be included in the heterostructure. In this study, we numerically investigate the effectiveness of the proposed structure for a highly efficient DFG-THz source with an ultrasmall footprint.

2. Numerical simulations

The integrated PhC-WGs designed for the numerical simulations are shown in Fig. 1 (upper). Based on a common straight PhC-WG formed with a missing line of air holes, the heterostructure consists of an LVLD PhC-WG for DFG connected with two STD PhC-WGs (STD PhC-WG1 and 2) to introduce fundamental light (signal and pump). The angular frequencies of these lights (ω_1 and ω_2) were set at 1.55 μm band in wavelength, and the frequency difference between them was set to 1 THz. To suppress the two-photon absorption of each fundamental light, $Al_{0.26}Ga_{0.74}As$ (bandgap energy of 1.78 eV[26]) was used as the semiconductor slab material.[27] The material nonlinear parameter ($\chi^{(2)} = 47\,\mathrm{pm\,V^{-1}}$) was included in the numerical simulations.

The slab was perforated with 2D periodic air-hole arrays, with the structural parameters of lattice constant (a) and radius (r) defined as the ratio of the lattice constant (r/a). The lattice constant and value of r/a for LVLD PhC-WG were set at 359 nm and 0.31, respectively, because these values are suitable for matching the fundamental light wavelength with

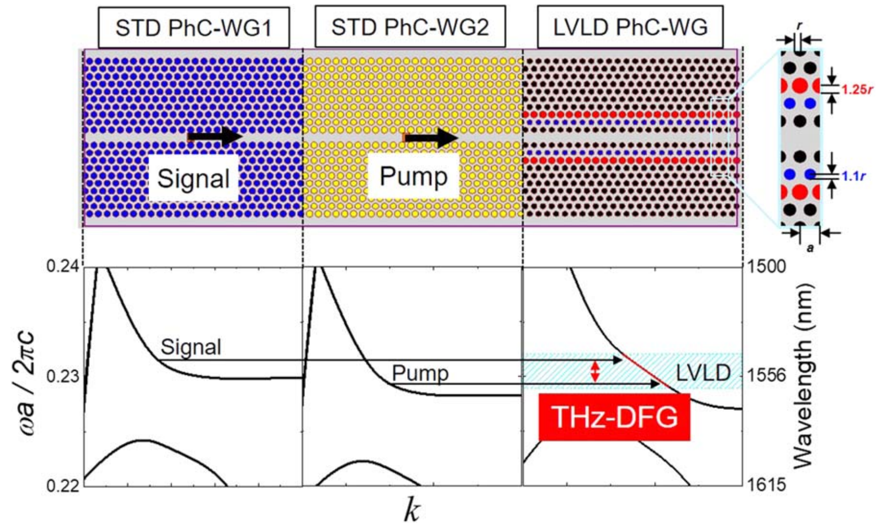

Fig. 1. (Color online) Schematic of the heterostructure of integrated PhC-WGs (upper) and the photonic band structure for each PhC-WG (lower).

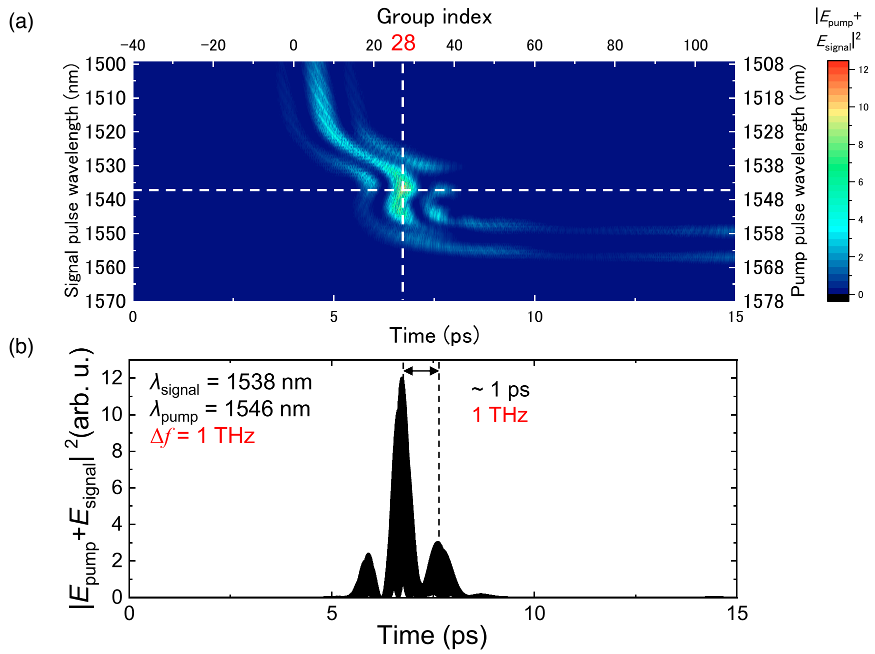

Fig. 2. (Color online) (a) Temporal power spectra of wave packets overlapped fundamental pulses with various wavelengths summarized in a heatmap. (b) Spectrum with the highest peak power obtained from optimal signal ($\lambda = 1538$ nm) and pump ($\lambda = 1546$ nm) pulses.

a 1.55 μm band, as previously reported.[17] In addition, the radii of air holes in the second and third rows from the WG were modulated to 1.1 and 1.25 times greater than the radius of other air holes, respectively, to obtain the LVLD mode for propagating fundamental light.

The photonic bands of the LVLD and STD PhC-WGs were calculated using the plane-wave expansion method, as shown in the lower panel of Fig. 1. Although the detailed procedure is described in the following section, the photonic bands in STD PhC-WG1 and 2 were designed for each fundamental light to be slow-light, and the bands were shifted from each other by varying the values of r/a in STD PhC-WG1 and 2. The slowed fundamental light can be highly coupled with the LVLD PhC-WG mode owing to the reduced group index difference. In addition, the shift of the STD PhC-WG1 band to a shorter wavelength than that of the STD PhC-WG2 band enables the fundamental light coupling to the photonic band in the next PhC-WG to the right, whereas it cannot be coupled to the other direction, owing to the absence of optical modes in that direction.[23] Therefore, the coupling efficiency of fundamental light in the LVLD PhC-WG can be increased.

The electromagnetic waves of the signal and pump lights (pulsed and continuous-wave) were launched from the centers of the regions of the STD PhC-WG1 and 2, respectively, and their propagation was numerically simulated using the finite-difference time-domain (FDTD) method. Temporal intensity variations were detected using a monitor set across the WG. For comparison, a similar simulation was performed for the structure in which the LVLD PhC-WG was replaced with a strip WG of AlGaAs with identical width and length. To investigate the DFG intensity qualitatively, the temporal power spectra were Fourier-transformed to measure the intensity spectrum in the frequency domain.

3. Results and discussion

First, we simulated the wave packets formed in the LVLD PhC-WG by overlapping fundamental light pulses with various wavelengths while maintaining a frequency difference of 1 THz. Figure 2(a) summarizes the temporal power spectra of the electric fields overlapped pulses ($|E_{\mathrm{pump}} + E_{\mathrm{signal}}|^2$) propagated through the LVLD PhC-WG in the heatmap with variations in the signal and pump pulse wavelengths. Figure 2(b) shows the spectrum of the wave packet when two wavelengths of 1538 and 1546 nm were used for the signal and pump pulses, respectively. In the wave packet, temporal oscillation was observed for a period of approximately 1 ps. This could be caused by the DFG, where the frequency difference was set to 1 THz. The peak power of oscillation was the highest among the various wavelengths of fundamental light, where the group refractive index was approximately 28, as indicated by the white dashed lines in Fig. 2(a). Since then, we have utilized these wavelengths for the fundamental light introduced into the LVLD PhC-WG.

Next, the pulse propagations of the fundamental light in the heterostructure were simulated to determine the optimal values of *r*/*a* for the STD PhC-WG1 and 2. While varying the value of *r*/*a* of each STD PhC-WG, the propagation of pulsed light (1 ps duration) was simulated to estimate the actual group velocities (v_g) of the fundamental light in the integrated PhC-WGs. Fundamental light with shorter (signal) and longer (pump) wavelengths was launched from STD PhC-WG1 and 2, respectively. The temporal power of the propagated pulses was measured using monitors #1–4, as shown in Fig. 3(a). When the value of *r*/*a* of each STD PhC-WG was increased, the photonic band shifted upward (higher frequency), and the value of v_g of the fundamental light with a fixed wavelength decreased (i.e., the group index (n_g) for the fundamental light increased). The increase in n_g is preferable to reducing the difference in n_g between the STD and LVLD PhC-WGs, resulting in an improvement in coupling efficiency. However, an excessive decrease in n_g causes a pulse chirp owing to the dispersion of the photonic band. Therefore, we determined the value of *r*/*a* of each STD PhC-WG to maximize n_g for each fundamental light just before the appearance of the pulse chirp: 0.325 for the signal pulse (STD PhC-WG1) and 0.320 for the pump pulse (STD PhC-WG2).

The power spectra of the signal and pump pulses propagating through the structurally optimized STD and LVLD PhC-WGs are presented in Figs. 3(b) and 3(c), respectively. By measuring the transit time of their peaks between the monitors, the v_g and n_g in each PhC-WG region for the fundamental lights were determined. The n_g values for the signal pulse were approximately 23, 16, and 28 for the STD PhC-WG1, 2, and LVLD PhC-WG, respectively. The n_g values for the pump pulse were approximately 22 and 28 for STD PhC-WG2 and LVLD PhC-WG, respectively.

From these n_g values, the transmittance of the signal pulse estimated using the Fresnel equation was 0.974 at the boundary between the regions of STD PhC-WGs 1 and 2 and 0.928 at the boundary between STD PhC-WG2 and LVLD PhC-WG. The estimated transmittance of the pump pulse was 0.928 at the boundary between STD PhC-WG2 and LVLD PhC-WG. Thus, the estimated coupling efficiencies of the signal/pump pulses in the LVLD PhC-WG were 0.904 and 0.928, respectively. In addition, we evaluated the actual coupling efficiencies based on the peak power of the pulses using FDTD simulations. The coupling efficiencies of the signal and pump pulses in the LVLD PhC-WG were 0.902 and 0.914, respectively. These values correspond well with the transmittance values calculated from n_g values. Considering that the estimated coupling efficiency of the LVLD PhC-WG from air was 0.133, the coupling loss due to the reflection at the boundary of the LVLD PhC-WG can be drastically lowered (approximately one-seventh) by using the heterostructure, demonstrating the effectiveness of the proposed heterostructure.

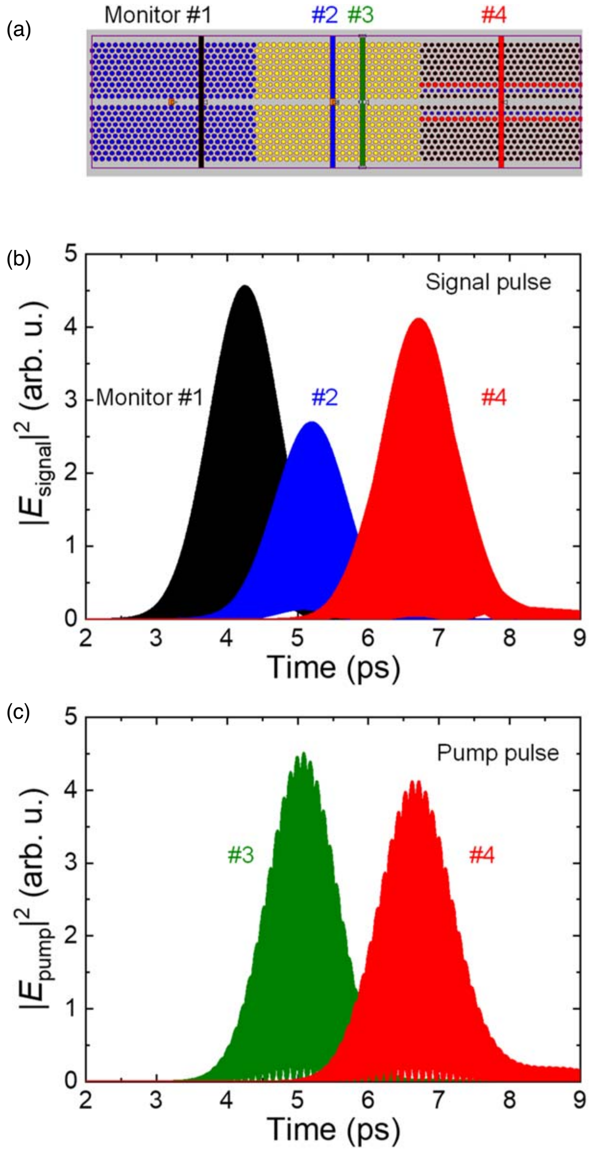

Fig. 3. (Color online) (a) Schematic of the integrated PhC-WGs and time monitors set across the WG. Simulated temporal power spectra of propagating (b) signal and (c) pump pulses.

Based on the propagation results, we set the launch times of the signal and pump pulses such that the pulses overlap in the LVLD PhC-WG and strip WG. The temporal power spectra measured at the end of the LVLD PhC-WG and the strip WG are compared in Fig. 4(a). In both models, a temporal oscillation corresponding to 1 THz was observed in

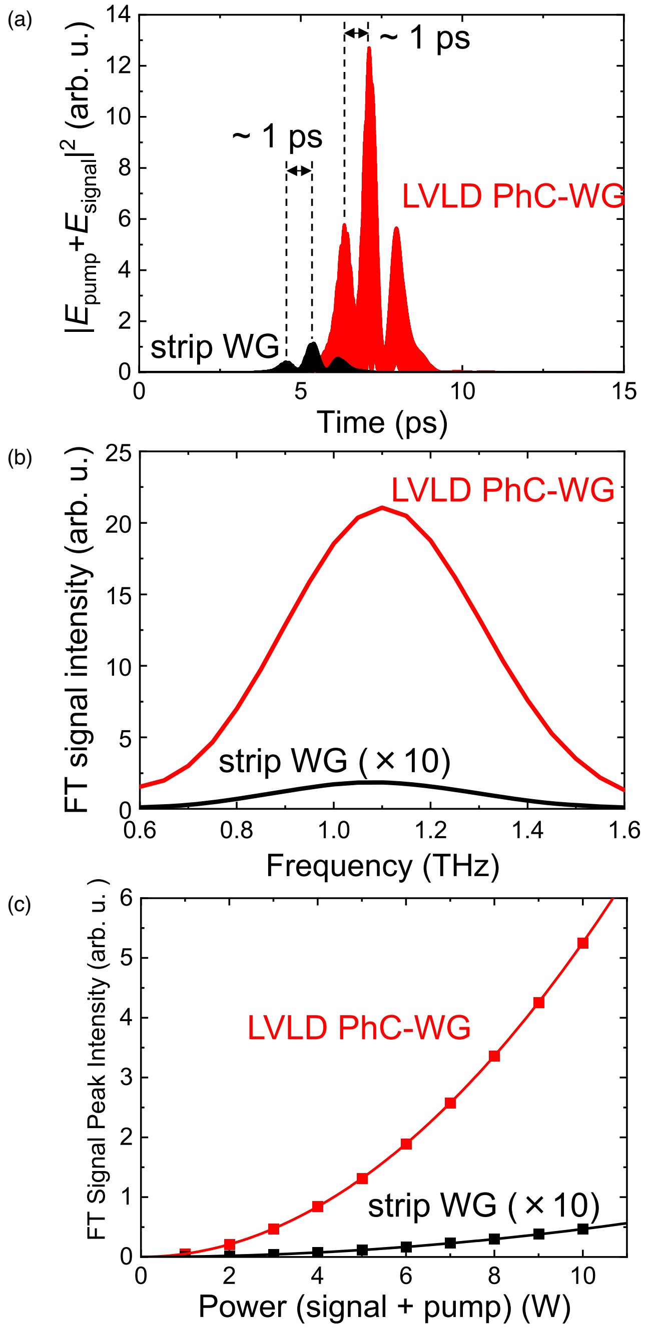

Fig. 4. (Color online) Comparison between the LVLD PhC-WG and AlGaAs strip WG: (a) temporal pulsed power spectra and (b) Fourier-transformed spectra. (c) Dependence of the Fourier-transformed signal peak intensity on the input power of the signal and pump pulses.

the wave packet, suggesting a DFG. The peak power obtained from the LVLD PhC-WG was approximately 11 times higher than that obtained from the strip WG. This can be attributed to the enhancement of the two pulses within the LVLD PhC-WG owing to low-group velocity and low-dispersion. To quantitatively compare the DFG intensities, the time function of the light intensity was Fourier-transformed. A comparison of DFG intensities is shown in Fig. 4(b). The peak intensity of the heterostructure with the LVLD PhC-WG was approximately 114 times higher than that of the heterostructure with the strip WG. This enhancement can be attributed to the increased coupling efficiency and n_g of LVLD PhC-WG, by considering that the DFG enhancement depends on the square of n_g.[17] In addition, we investigated variations of the Fourier-transformed intensity as a function of input power of fundamental light. As shown in Fig. 4(c), the intensity increases quadratically as a function of the input power of the signal and pump pulses. These results demonstrate the nonlinear DFG enhancement in the LVLD PhC-WG. On the other hand, the peak frequency of the Fourier-transform spectra was slightly shifted from 1 THz, and the linewidth of the spectra broadened. This could be due to the limited pulse duration of the fundamental light, which did not cause sufficient interference between the fundamental light.

Then, we introduced continuous-wave fundamental lights for numerical simulations. Figure 5(a) shows the intensity variations measured on a monitor set at the end of the PhC-WG (indicated by the red line) and strip WG (indicated by the black line). The intensity gradually increased and remained stationary after several ps. Sufficient time of interference between the fundamental lights exhibited a constant temporal oscillation in both WGs, and the oscillation period was close to 1 ps. The Fourier-transform spectra shown in Fig. 5(b) also indicate that the peak frequency corresponded well with 1 THz, and the linewidth was narrower than that of pulsed light. The peak intensity through the LVLD PhC-WG was approximately 136 times that through the strip waveguide. The DFG coherency increased over that of the pulsed light, which could enhance the ratio of

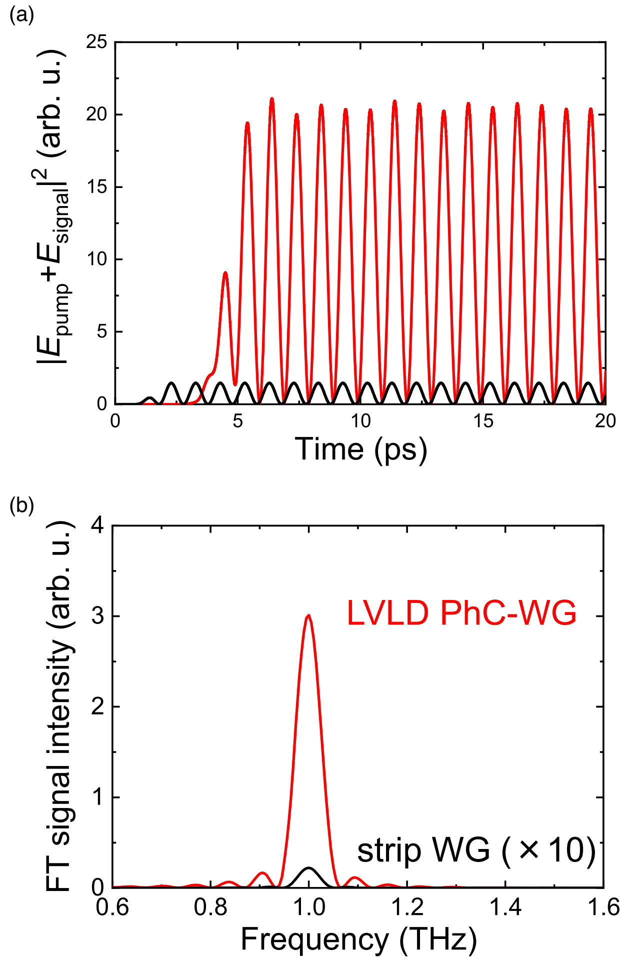

Fig. 5. (Color online) Comparison between LVLD PhC-WG and AlGaAs strip WG: (a) temporal CW power spectra and (b) Fourier-transformed spectra.

the Fourier-transform intensity between the LVLD PhC and strip WGs.

From the above results, the proposed heterostructure was demonstrated to have potential for application in THz light sources with a smaller size and more efficient DFG than conventional materials. For practical fabrication of the THz source, light-emitting materials in STD PhC-WG1 and 2 can be realized by embedding quantum wells or dots in the semiconductor slab, as we previously demonstrated.[23,28,29] In addition, the selective-area growth technique developed for integrated PhC-WGs[30,31] can be applied to the heterostructure to avoid reabsorption of the fundamental light in LVLD PhC-WG. Using these techniques, highly efficient DFG-THz sources based on integrated PhC-WGs with ultrasmall footprints may be feasible.

4. Conclusions

A heterostructure integrating two STD PhC-WGs and an LVLD PhC-WG was developed for highly efficient DFG-THz sources and was verified by numerical simulations. The temporal power spectra propagating light measured a peak intensity more than 10 times higher, and the peak intensity of FT signal was more than 100 times higher than that of strip WG. These results indicate that the proposed heterostructure has the potential to be applied to ultrasmall and highly efficient THz sources.

Acknowledgments

This study was partly supported by JSPS KAKENHI (20K21005).

ORCID iDs

Nobuhiko Ozaki https://orcid.org/0000-0002-3890-7842

1) D. Molter et al., Appl. Sci. **11**, 950 (2021).
2) K. Kawase, Y. Ogawa, and Y. Watanabe, Opt. Express **20**, 2549 (2003).
3) M. Hangyo, Jpn. J. Appl. Phys. **54**, 120101 (2015).
4) A. E. Willner, X. Su, H. Zhou, A. Minoofar, Z. Zhao, R. Zhang, M. Tur, A. F. Molisch, D. Lee, and A. Almaiman, J. Opt. **24**, 124002 (2022).
5) L. Schrottke, X. Lu, K. Biermann, P. Gellie, and T. Grahn, AIP Adv. **12**, 085122 (2022).
6) Y. Takida, K. Nawata, S. Suzuki, M. Asada, and H. Minamide, Opt. Express **25**, 5389 (2017).
7) M. Tonouchi, Nat. Photon. **1**, 97 (2007).
8) W. Li, F. Qi, P. Liu, Y. Wang, and Z. Liu, Opt. Lett. **47**, 178 (2022).
9) Y. Liu, K. Zhong, A. Wang, M. Zhou, S. Li, L. Gao, and Z. Zhang, Crystals **12**, 936 (2022).
10) Z. B. Zaccardi, I. C. Tangen, G. A. Valdivia-berroeta, C. B. Bahr, K. C. Kenney, C. Rader, M. J. Lutz, B. P. Hunter, D. J. Michaelis, and J. A. Johnson, Opt. Express **29**, 38084 (2021).
11) J. Kuttruff, M. V. Tsarev, and P. Baum, Opt. Lett. **46**, 2944 (2021).
12) X. Yin, S. Fan, X. Zhang, Y. Li, Z. Liu, X. Zhao, and J. Fang, Opt. Express **30**, 21797 (2022).
13) A. V. Ovchinnikov, O. V. Chefonov, M. B. Agranat, M. Shalaby, and D. S. Sitnikov, Opt. Lett. **47**, 5505 (2022).
14) H. T. Olgun et al., Opt. Lett. **47**, 2374 (2022).
15) T. Tanabe, K. Suto, J. Nishizawa, K. Saito, and T. Kimura, Appl. Phys. Lett. **83**, 237 (2003).
16) K. Saito, T. Tanabe, and Y. Oyama, Opt. Express **22**, 16660 (2014).
17) T. Nakahama, N. Ozaki, H. Oda, N. Ikeda, and Y. Sugimoto, Jpn. J. Appl. Phys. **59**, 090903 (2020).
18) N. Ikeda, Y. Sugimoto, Y. Watanabe, N. Ozaki, Y. Takata, Y. Tanaka, K. Inoue, and K. Asakawa, Opt. Commun. **275**, 257 (2007).
19) K. L. Vodopyanov, Laser Photonics Rev. **2**, 11 (2008).
20) K. Inoue and K. Ohtaka (ed.) *Photonic Crystals* (Springer, Berlin, 2004).
21) T. Baba, Nat. Photon. **2**, 465 (2008).
22) C. Monat, B. Corcoran, M. Ebnali-Heidari, C. Grillet, B. J. Eggleton, T. P. White, L. O'Faollain, and T. F. Krauss, Opt. Express **17**, 2944 (2009).
23) S. Uchida, N. Ozaki, T. Nakahama, H. Oda, N. Ikeda, and Y. Sugimoto, Jpn. J. Appl. Phys. **56**, 050303 (2017).
24) S. Kubo, D. Mori, and T. Baba, Opt. Lett. **32**, 2981 (2007).
25) N. Ozaki, Y. Kitagawa, Y. Takata, N. Ikeda, Y. Watanabe, A. Mizutani, Y. Sugimoto, and K. Asakawa, Opt. Express **15**, 7974 (2007).
26) M. E. Allali, C. B. Soensen, E. Vaje, and P. T-Peterson, Phys. Rev. B **48**, 4398 (1993).
27) H. Oda and K. Inoue, Appl. Phys. Lett. **90**, 231102 (2007).
28) H. Oda, A. Yamanaka, N. Ozaki, and Y. Sugimoto, AIP Adv. **6**, 065215 (2016).
29) K. Inoue, H. Sasaki, K. Ishida, Y. Sugimoto, N. Ikeda, Y. Tanaka, S. Ohkouchi, Y. Nakamura, and K. Asakawa, Opt. Express **12**, 5502 (2004).
30) N. Ozaki, Y. Takata, S. Ohkouchi, Y. Sugimoto, Y. Nakamura, N. Ikeda, and K. Asakawa, J. Cryst. Growth **301–302**, 771 (2007).
31) N. Ozaki, Y. Takata, S. Ohkouchi, Y. Sugimoto, N. Ikeda, and K. Asakawa, Appl. Surf. Sci. **254**, 7968 (2008).